Defence Science Journal, Vol. 74, No. 4, July 2024, pp. 428-438, DOI : 10.14429/dsj.74.19352

A Novel Method to Estimate Base Drag and Burn Time from Flight Data Using Extended Kalman Filter

L.K. Gite* and R.S. Deodhar

DRDO-Armament Research & Development Establishment, Pune - 411021, India
**E-mail: lkgite.arde@gov.in*

ABSTRACT

Estimating highly spinning projectiles' base drag and burn time by static trials is challenging. Drag profiles obtained using numerical methods or experimental or wind tunnel estimations should be updated using the estimates obtained from dynamic flight test data. This paper proposes a novel methodology to estimate the base drag and burn time from flight data using an extended Kalman Filter. Trajectory positional data is used to calculate base drag and indirect measurement of burn time. The simulation is carried out for two cases, artillery shell and rocket. The proposed method works well for both cases. Exhaustive simulation results indicate that the technique can be used for any configuration. Estimating both base drag and burn time is within 5 % accuracy.

Keywords: Base drag; Burn time; Extended Kalman filter; Modified point mass model

NOMENCLATURE

x	: Horizontal distance (Range), m
y	: Lateral distance (Drift), m
z	: Vertical distance (Height), m
d	: Diameter of projectile, m
m	: Mass of projectile, kg
Ix	: Axial moment of inertia, kg m^2 ρ
ρ	: Density of air, kg/m^3
sp	: Roll rate, rad/s
v	: Projectile speed, m/s
t	: Time, s
V_x,V_y,V_z	: Air velocity components, m/s
u_x,u_y,u_z	: Projectile velocity components, m/s
c_x,c_y,c_z	: Coriolis acceleration components, m/s^2
g_x,g_y,g_z	: Gravitational acceleration components, m/s^2
T_x,T_y,T_z	: Thrust acceleration components, m/s^2
W_x,W_y,W_z	: Wind velocity components, m/s
$\ddot{x}, \ddot{y}, \ddot{z}$	: Projectile acceleration components, m/s^2
T_s	: Sampling time, s
m_x,m_y,m_z	: Components of yaw of repose
μ_s	: Process noise
C_D	: Drag force coefficient
$C_{D_{bo}}$	: Base drag coefficients
f_{dr}	: Base drag coefficient factor
$C_{L\alpha}$	: Lift force coefficients
$C_{L\delta}$	: Roll coefficient due to the CA angle
C_{lp}	: Roll damping coefficient
$C_{\gamma p_\alpha}$	: Magnus force coefficient
$C_{M\alpha}$	: Pitching moments coefficient
x	: System state vector
f(x)	: Nonlinear function of states
w	: Random zero mean process noise
z	: Measurement state vector
h(x)	: Measurement Eqn.
v	: Random zero mean measurement noise
I	: Identity matrix
$\bar{\mathbf{x}}_k$	: Estimate obtained from system dynamics
$\hat{\mathbf{x}}_k$	: Updated estimates
Q	: Random zero mean process noise R
R	: Random zero mean measurement noise F
F	: Jacobian of system dynamics H
H	: Jacobian of measurements
M	: Error covariance matrix before update
P	: Error covariance matrix after update
K	: Kalman gain matrix
x′, y′, z′, sp′	: Actual measurements
$\delta_x,\delta_y,\delta_z,\delta_{sp}$	: Gaussian noise in the measurement

Received : 11 August 2023, Revised : 11 December 2023
Accepted : 12 March 2024, Online published : 24 July 2024

1. INTRODUCTION

The trajectory of artillery projectiles, rockets, and mortar bombs depends primarily on the mass, diameter, and inertia of projectiles, launching conditions and atmospheric conditions and aerodynamic parameters like drag. The total drag acting on a projectile can be divided into three components: pressure, dense and base. When the projectiles move in the air, the airflow cannot return quickly enough to fill the space behind the projectile, creating a region of low pressure immediately behind the projectile. Due to intense pressure at the base, a vacuum or suction effect generates a resistance to motion. The resistance produced by the suction effect at the base of the projectile is

called base drag. The relative magnitude of aerodynamics drag components are 20 % pressure drag, 30 % viscous drag, and 50 % base drag[1]. Hence, base drag is a significant component of the total drag. Therefore, minimization of the base drag is essential to reach the maximum range or to achieve higher terminal velocity. The analysis of various components of drag is crucial in the preliminary design stage of a shell or a rocket and it can aid the designer in finding potential areas for drag reduction[2].

To reduce base drag as much as possible, putting a 'boattail' on the rear of the shell is desirable. A boattail is a frustum of a cone designed to entrain the boundary layer into the base region of the artillery shell. Another way to reduce base drag is to generate gas into the base region of a projectile in-flight by burning a small quantity of fuel fitted into the rear of the projectile. This technique is known as Base Bleeding (BB).The propellant burns at low pressure and generates a jet of gas at the base, increasing the pressure behind the projectile base and reducing base drag by up to 50 % due to a reduction in base drag range increases of up to 30 %[3]. BB units are widely used as a means of projectile drag reduction to extend the range of artillery shells.

The BB units are usually subject to high spin rates and changes in velocities and ambient atmospheric pressures at every instance. Burn rate increases due to spin and decreases in higher ambient pressure[4]. Standard lump sum models for gas generation usually achieve good predictions for total burn time under these varying conditions, especially if erosive burning underspin is considered. However, it has proven difficult to predict observed BB active drag accurately in practice. Fitting functions need to be introduced, which need to be determined from extensive test firings. Therefore, a reliable model predicts BB burn time and drag with good accuracy and minimal input number of parameters[5]. The flow out of the base bleed is subsonic, which means that the internal ballistics of the base bleed unit are coupled to the external base pressure. Base pressure controls the base drag. The coupling between base drag and base bleed internal ballistics is often given through empirical expressions due to a need for more understanding of viscous-inviscid flow interactions between a near-wake flow and a freestream[6]. Little is known about the fluid dynamic processes inside the unit and the base flow region. BB units are, therefore, mainly designed empirically, using extensive and expensive test firings to estimate the drag reduction.

For a slowly spinning fin-stabilized rocket, the base flow in the power phase has complex fluid dynamic behaviour involving separated flows, free-shear layers, high levels of turbulence, and strong shock waves and expansions, which may be subject to interference effects. The situation may be further complicated by additional chemical and thermal effects[7]. Prediction of power-on base drag is a very critical part of overall drag. Estimating the power of the base drag component for a given geometry and propulsion unit $\frac{p_b}{p_\infty}$ is essential.

The average base pressure and free stream pressure ratio are essential to estimate base drag. Many approximations are developed to predictand used to compute the base drag coefficient and drag reduction factor. Improved methods for base pressure prediction under base bleed and rocket motor-on conditions have been developed[8]. All these methods are either based on approximation or numerical computation.

Many researchers and designers suggested a correlation law to estimate the base drag of bodies of revolution with a central jet exhaust at the base. Improved correlation laws were proposed and implemented. Aero prediction code is a commercial code that can estimate the base drag of missiles, rockets and projectiles at supersonic and transonic speeds.

The past few years have witnessed widespread application of various techniques, e.g., semi-empirical based models and computational fluid dynamics (CFD) methods, etc., for providing flow field details. The difficulties in determining full-scale nonlinear flow effects from subscale wind tunnel test data are some factors that impose limitations on using wind tunnels in routine flight analysis. Further to theoretical estimates, a ground test spin fixture was used to obtain measurements in the base region of the projectile. However, there are still limitations to building and operating test facilities changing altitude pressure as experienced by projectiles[9]. To model base flow, support at the wing tip, which restricts spin, is required. Base drag measurement with spin and changing surrounding pressure is almost impossible. Thus, the practical problems in using wind tunnel tests for this estimation, the data complexity, and the high computational costs of the CFD methods are functional limitations. Consequently, analysis guided by flight data for parameter estimation is the best recourse[10].

There are methods to improve the initial estimation of aerodynamic coefficients. The resistance coefficient is identified in each step to correct aerodynamic parameters in the missile space motion model[11-12]the optimal dynamic fitting method was successfully applied to an optimal tracking control problem, namely aerodynamic curve identification from flight testing data. An iterative learning identification method is proposed to extract a projectile's optimal fitting drag coefficient curve from radar-measured velocity data[13]. The extended high-order iterative learning identification scheme effectively applies to practical curve identification problems[14].

The extended Kalman Filter technique estimates two major unknown factors: manoeuvrable acceleration and ballistic coefficient of re-entry targets[15].

To estimate the trajectory state parameters and accurate impact point, a prediction method is proposed[16]. EKF is used to precisely reconstruct the state's position, velocity, acceleration, and ballistic coefficient of high-speed re-entry targets. The estimation of manoeuvrable accelerations has also been explored[17].

An improved hybrid extended Kalman filter is proposed for drag coefficient estimation from flight data of projectiles. The unknown constant parameters to be identified are obtained in[18]. The GPS measurements of the absolute position can also be used as measurements. Extended Kalman filtering is used to extract wind profile[19]. EKF is used to estimate the yaw angle at each point on the trajectory from the flight data[20]. The method uses an extended Kalman filter, and system dynamics are modelled using a modified point mass trajectory model.

It is a routine practice to capture the trajectories of these projectiles in motion using a ground-based tracking radar system. Generally, typical trajectory data of a projectile in motion, acquired by tracking radar, contain measurements

of trajectory variables, namely range (x), height (z), and drift (y). This trajectory data could effectively be processed using an appropriate estimation algorithm to estimate a few aerodynamic parameters of the artillery projectile in motion. Given the availability of primary trajectory data, a method of estimation of base drag from flight data will be helpful.

Section 2 of this paper briefly introduces the Extended Kalman Filter, the approach for estimating base drag, and the system dynamics model used for trajectory computation. Section 3 presents the base drag estimation results obtained with the proposed approach for spin-stabilized shells and rockets. The method of burn time estimation is demonstrated in Section 4. Section 5 concludes the paper.

2. PROBLEM FORMULATION AND SYSTEM DYNAMICS

2.1. Extended Kalman Filter

For the application of the Extended Kalman Filter (EKF), the system is expressed in the state space form as given by Eqn. (1)

$$\dot{x} = f(x) + w \tag{1}$$

A vector f representing the system's state is a nonlinear function of the state and is a random zero mean process noise w. The process noise matrix describing the process is given $Q=E[ww^T]$ a covariance matrix of the noise.

In EKF, the measurement Eqn. connecting state and measurements is also considered nonlinear and given by Eqn. (2).

$$z = h(x) + v \tag{2}$$

where, v is zero mean random process representing measurement noise with covariance matrix given by $R=E[vv^T]$

For application purposes, a discrete version of EKF is used. At k^{th} time instant, let the state be represented by x_k and measurement be z_k. Let the estimate of the state at k^{th} time instant, obtained from propagating the state estimate at $(k-1)^{th}$ instant, be denoted by $\overline{\mathbf{x}}_\mathbf{k}$. After updating with the help of measurement, the state's estimate z_k is represented by $\hat{\mathbf{x}}_\mathbf{k}$ and obtained using the integration of the system dynamics Eqn. using the Runge Kutta Method.

The system Eqn. governing the projectile are highly nonlinear, and the observation Eqn. are also nonlinear. Let $f=(f_1,f_2,\ldots,f_n)$ be system dynamics Eqn. and measurement dynamics Eqn. The Riccati Eqn. system and measurement dynamics matrices are used to calculate filter gain. The filtering process uses the Jacobian F of the system dynamics and the Jacobian H of the measurement Eqn.s. These matrices will be calculated at each timestep and used by the filter to update the estimates of the state variables. The Jacobian of the system is calculated by taking partial derivatives of each of the state Eqn.s concerning each of the state variables.

The first-order approximations of system and measurement Eqn.sare used to obtain the system dynamics matrix and measurement matrix H. And are given by Eqn. (3) and Eqn. (4), respectively. When the state estimate is $\hat{x}$,

$$F = \left.\frac{\partial f(x)}{\partial x}\right|_{x=\hat{x}} \tag{3}$$

and

$$H = \left.\frac{\partial h(x)}{\partial x}\right|_{x=\hat{x}} \tag{4}$$

The fundamental matrix, which in general is used for propagating the state forward by time t, is obtained using Taylor's series expansion as given in Eqn. (5)

$$\Phi(t) = e^{Ft} = 1 + Ft + \frac{(Ft)^2}{2!} + \ldots \tag{5}$$

When t, i.e., the time step is small, then Eqn. (5) can be approximated to Eqn. (6)

$$\Phi(t) \approx 1 + Ft \tag{6}$$

This paper is used to calculate Kalman gain, which controls the amount of correction to be made in the estimation.

The Ricatti Eqn. (7) to Eqn. (9) required for obtaining Kalman gain at k^{th} time instant are given as follows.

$$M_k = \Phi_k P_{k-1} + \Phi_k^T + Q_k \tag{7}$$

$$K_k = M_k H^T (H M_k H^T + R_k)^{-1} \tag{8}$$

$$P_k = (I - K_k H) M_k \tag{9}$$

where, is the covariance matrix representing errors in the state estimate before the update, and P_k is the covariance matrix representing errors in the state estimate after the update? Matrix K_k represents the Kalman gain and Φ_k is a fundamental matrix when the state estimate is $\overline{x}_k$ If the time step or sampling time is T_s, then the discrete process noise matrix $Q_k$is obtained using Eqn. (10)

$$Q_k = \int_0^{T_s} \Phi(\tau) Q \Phi(\tau)^T d\tau \tag{10}$$

In the matrix, the covariance of the measurement noise is characteristic of the sensors used for measurement. This matrix may remain constant throughout the filtering process or depend on the current state. In this work, we assume it to be stable.

Now, in EKF, the estimate $\overline{x}_k$ obtained from system dynamics is updated with the help of measurement vector using Eqn. (11)

$$\hat{x} = \overline{x}_k + K_k[z_k + h(\overline{x}_k)] \tag{11}$$

This new estimate is expected to be more accurate state of the system as measurements are used to update prediction obtained from the system model and given by Eqn. (12).

$$\overline{x}_k = \hat{x}_{k-1} + f(\hat{x}_{k-1}) T_s \tag{12}$$

For each time step of the filter, the states and error covariance matrix are first propagated according to the system dynamic model and dynamic noise.

2.2 System Dynamic and the Proposed Approach

If the projectile has good dynamic stability, the Modified Point Mass (MPM) model can approximate the projectile's motion. MPM model is a conventional point mass model with an axial roll and instantaneous equilibrium yaw term added to it. The MPM considers accelerations due to drag, lift, Magnus force, Coriolis force, and gravity. It estimates the angle of yaw, drag, drift, and Magnus force effects resulting from yaw of repose. Drag, lift, Magnus force coefficient, and pitch and roll damping coefficients are aerodynamic inputs to the model. It has been proved that the modified point mass model accurately calculates trajectories of roll stabilized, slowly rolling, and finned projectiles.

To estimate, we have considered the state of the system as it is assumed that all the system dynamics parameters except the drag coefficient are known or measured. In addition, if we believe that the drag coefficient μ is constant concerning time, that means its derivative must be zero, i.e.. However, the new state component requires an additional process noise

component since the drag coefficient of the projectile may have an error since it is not modelled precisely in system dynamics. The drag coefficient can be described as the function of a Mach number and other parameters. To account for the fact that the drag coefficient may vary and to make the resultant filter more robust we can add process noise to the derivative of the drag coefficient. Therefore, the Eqn. for the derivative of the ballistic coefficient becomes where is process noise.

It is known that the filter's performance strongly depends on the motion model. Hence, system dynamics, including the most essential forces and moments, can be adopted for better results. The tuned Modified Point Mass model is selected as system dynamics since the Modified Point Mass model after appropriate tuning, and 6 DOF give equivalent results as reported in[21]. For the study, input trajectory data available for estimation is range (x), drift (y), height (z), and spin rate (sp)considered. Given the availability of input data and the capability of MPM compared to 6 DOF, it is adequate to use MPM as system dynamics to estimate the base drag and time of flight. It is necessary to convert the point mass trajectory differential Eqn. into state space form to apply an extended Kalman filter.

The projectile positions range, line and height, spin, respective velocities, and drag coefficient to be estimated are represented as state vector $\mathbf{x} = [x, y, z, sp, \dot{x}, \dot{y}, \dot{z}, \mu = CD]^T$ Then modified point mass(MPM) trajectory model in state space form is $\dot{x} = f(x) + w$ given by Eqn. (13)

$$\begin{bmatrix} \dot{x} \\ \dot{y} \\ \dot{z} \\ \dot{p} \\ \ddot{x} \\ \ddot{y} \\ \ddot{z} \\ \dot{\mu} \end{bmatrix} = \begin{bmatrix} f_1 = u_x \\ f_2 = u_y \\ f_3 = u_z \\ f_4 = \frac{1}{I_x}\frac{\rho V^2}{2}\frac{\pi d^2}{4}\left(C_{l_d} + C_{lp}\frac{pd}{2v}\right)d \\ f_5 = \frac{\pi\rho d^2}{8m}\left[-C_D v(v_x - w_x) + C_{L_\alpha}\alpha_x v^2 - \frac{d}{2}C_{\gamma_{p\alpha}} pm_x\right] + T_x + c_x + g_x \\ f_6 = \frac{\pi\rho d^2}{8m}\left[-C_D v(v_y - w_y) + C_{L_\alpha}\alpha_y v^2 - \frac{d}{2}C_{\gamma_{p\alpha}} pm_y\right] + T_y + c_y + g_y \\ f_7 = \frac{\pi\rho d^2}{8m}\left[-C_D v(v_z - w_z) + C_{L_\alpha}\alpha_z v^2 - \frac{d}{2}C_{\gamma_{p\alpha}} pm_z\right] + T_z + c_z + g_z \\ f_8 = 0 \end{bmatrix} + \begin{bmatrix} 0 \\ 0 \\ 0 \\ 0 \\ 0 \\ 0 \\ 0 \\ \mu_s \end{bmatrix} \tag{13}$$

where, are projectile velocity components, v_x, v_y, v_z are air relative velocity components, w_x,w_y,w_z are wind velocity components, T_x, T_y, T_z thrust force components, c_x, c_y, c_z are Coriolis force components are yaw of repose components, $\ddot{x}, \ddot{y}, \ddot{z}$ are projectile acceleration components. Components are defined using yaw of repose and relative velocity. g_x,g_y,g_z are gravitational acceleration components. The velocity of the projectile is v, an axial moment of inertia I_x and μ_s denotes noise.

Here, the total drag coefficient, lift force coefficient C_{L_α}, Magnus force coefficient $C_{\gamma p_\alpha}$, and pitching moments coefficient C_{M_α} are primary aerodynamics coefficients used in MPM. It is assumed that the *m* mass of the projectile and *d* is the diameter of the projectile, and air density concerning height are known. The values during the ballistics phase and boost or base bleed phase differ.

MPM will compute the trajectory elements, i.e., range, drift, and height, at every time step. Using Cartesian to spherical transformations, these will be transformed into angles. In the absence of actual flight measurement data, it can be generated by adding suitable noise to the model simulation output. Noise will be added into respective slant range, elevation, and azimuthal angles. Finally, these noisy slant ranges and angles will be converted into (x,y, z) representing radar measurements.

We assume process noise to be present in the unknown state variable $\mu=C_D$. The measurement vector is in state space form and can be written as Eqn. (14).

$$\begin{bmatrix} x \\ y \\ z \\ sp \end{bmatrix} = \begin{bmatrix} x' \\ y' \\ z' \\ sp \end{bmatrix} + \begin{bmatrix} \delta_x \\ \delta_y \\ \delta_z \\ \delta_{sp} \end{bmatrix} \tag{14}$$

where, denotes actual positions and spin and $[\delta_x, \delta_y, \delta_z, \delta_{sp}]^T$ is Gaussian measurement noise vector representing noise in respective coordinates.

The trajectory data is filtered using EKF. At each stage, a new state is estimated with the help of EKF. Thus, the state variable μ gives the drag coefficient value at each time instance. Combining this information with the speed at this specific instance, we can create a drag profile for the velocity profile the projectile has experienced.

2.3 Initialization and Tuning

To achieve objectives in designing the Kalman filter for a given application is a tricky job. Initialization and tuning of filters are open problems. The filter tuning varies from ad hoc through empirical to rigorous methods. In this work, the initial state is the average of the first few measurements for known states. This is possible since we are processing data offline. For the parameters that are used as augmented states or unobservable as unknown in the EKF, some computational and experimental results are available. It is necessary to make a proper choice, which is neither zero nor consisting of tremendous values, to obtain accurate estimates and uncertainty. It is assumed that an initial value in the filter is close to zero and later adaptively updates and estimates it. Usually, a good initial estimate can be obtained from the calibration of the measuring instrument. The more details on initialization are given in references 22-24.

The process noise matrix is defined as follows. Since it is assumed that the system dynamics Eqn. are well defined for known variables and process noise is present only in unknown variables. We can assume the covariance between process noise of different state variables for other variables is zero i.e., $\sigma_{p_{ij}} = 0$ except i=j=8

$$Q = \begin{bmatrix} \sigma_{p_{11}} & \cdots & \sigma_{p_{18}} \\ \vdots & \ddots & \cdots \\ \sigma_{p_{81}} & \cdots & \sigma_{p_{88}} \end{bmatrix} \tag{15}$$

The measurement noise matrix R is defined as using $\sigma_{m_{ij}} = 0$ $\sigma_{m_{ij}}$ noise in respective measurement variables and their covariance i.e., $\sigma_{m_{ij}} = 0$ except i=j

$$R = \begin{bmatrix} \sigma_{p_{11}} & \cdots & \sigma_{p_{14}} \\ \vdots & \ddots & \cdots \\ \sigma_{p_{41}} & \cdots & \sigma_{p_{44}} \end{bmatrix} \tag{16}$$

The simulation is also carried out for different noise levels. It is assumed that the radar and launch point are collocated

Table 1. BB shell and rocket configurations

Parameters	Unit	Base bleed shell	Rocket
Stability	-	Spin	Fin
Configuration type	-	Shell	Rocket
Diameter	m	0.155	0.122
Total length	m	0.8787	2.970
In flight mass	kg	47.00	46.5
Axial moment of inertia (boost / base bleed phase)	kg/m^3	0.1610	0.1499
Lateral moment of inertia (boost/ base bleed phase)	kgm^3	2.1061	41.18
Axial moment of inertia	kgm^3	0.1592	0.1238
Lateral moment of inertia	kgm^3	2.0367	33.43
Muzzle velocity	m/s	900	26.7
Thrust/burn time/	s	23 /26	5.6
Thrust	kgf	-	1018.7
Propellant mass	kg	0.8	19

and radar gives processed range, drift, and height data. Three different noise levels σ = 5m, 10m, and 15m were simulated to test the robustness of the proposed method. The results are presented for noise level σ = 10 m.

3. BASE DRAG ESTIMATION

Artillery projectiles are either spin-stabilized or fin-stabilized. In this paper, the proposed method is evaluated fortwo types of projectile configurations given in Table 1[25].

Gyroscopically stable configuration has very high spin rate and fin stabilized configuration is slowly spinning configuration. The assumed values of the mass, inertia and burn time etc. for both the configuration are given in Table 1.

3.1 Base Drag of Rocket

The simulation is carried out for a 122 mm rocket. Measurements are generated for launch angle 45°. It is assumed that velocity of rocket at launch is 26 m/s. The burn time is 5.67 s. Range achieved is 33.6 km and vertex height attended during flight is 11.3 km. Total flight time is 100.2 s. The maximum velocity at all burnt point is 1003 m/s in 5.67 s. The Mach number at launch is 0.076 and at all burnt points is

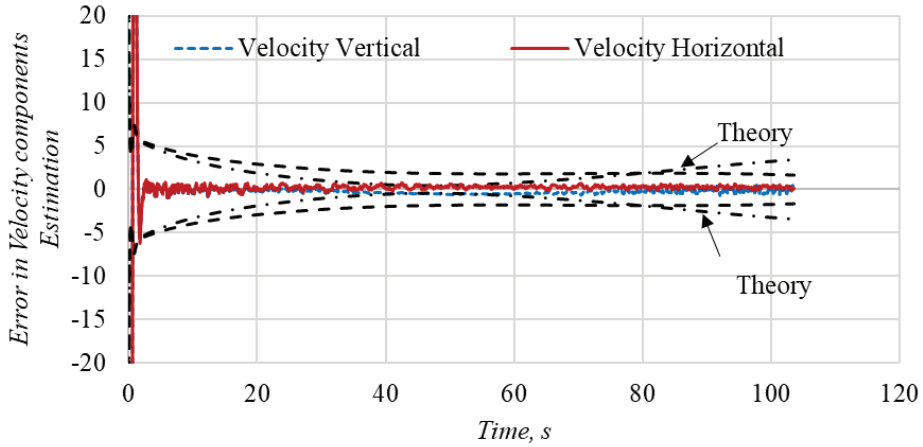

Figure 1. Errors in the estimated velocity components.

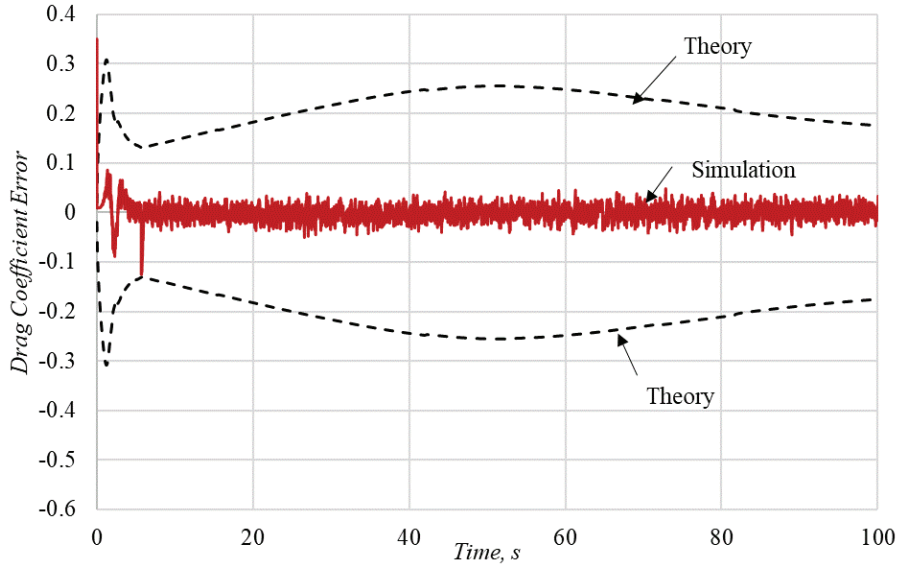

Figure 2. Errors in drag coefficient estimation and theoretical bounds.

2.95 and it reduces to Mach 1 along with the trajectory at the impact point.

The drag acting on the rocket during the boost phase is different and smaller since the rocket motor produces thrust opposite to drag. Hence, as such, there is no base drag component during the boost phase of the rocket. In this work, the drag during the boost and ballistics phase is estimated. Using these estimations, a reduction in total drag due to rocket mortar on can be obtained. The measurement data generated after adding a noise is passed to the developed EKF model.

The estimated velocity components are within theoretical bounds indicating that the filter is not diverging and are shown in Fig. 1.

The drag coefficient error and theoretical bounds of the drag coefficient estimated are shown in Fig. 2. The estimated drag profile concerning Mach no is shown in Fig. 3 and it can be inferred that the filter is following the drag profile.

Moreover, the mean of innovation, i.e., the difference between the measurement and predicted values. It is expected that the mean of innovation is close to zero for well well-performing filter. In this case, after settling the filter i.e., after 1/3 samples an innovation of range is calculated and it is 0.00086 indicating that the filter is performing well.

In the boost phase, the Mach number starts at 0.09 and increases and reaches 2.8 at all burnt points and decreases along with the ballistics phase of the trajectory.

It is observed that EKF can switch to ballistics phase coefficients automatically once measurements of the boost phase are over. The estimated base drag is compared with existing known drag values used to generate the trajectory, i.e., measurements in the respective phase. It is a direct comparison. The percentage error is calculated for both the estimated boost and ballistics phases. The percentage error is calculated for estimated boost and ballistics phase drag and is

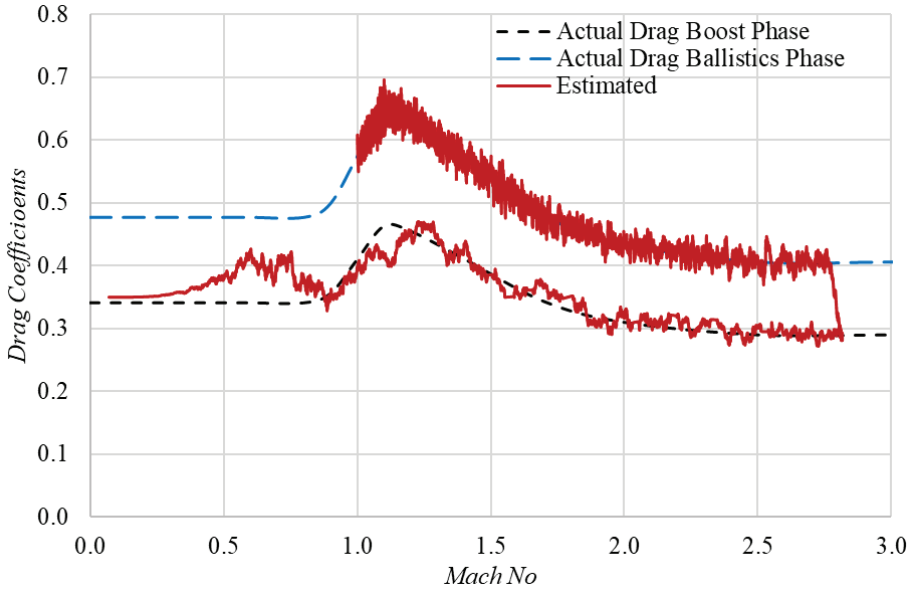

Figure 3. Boost and ballistics phase drag estimation.

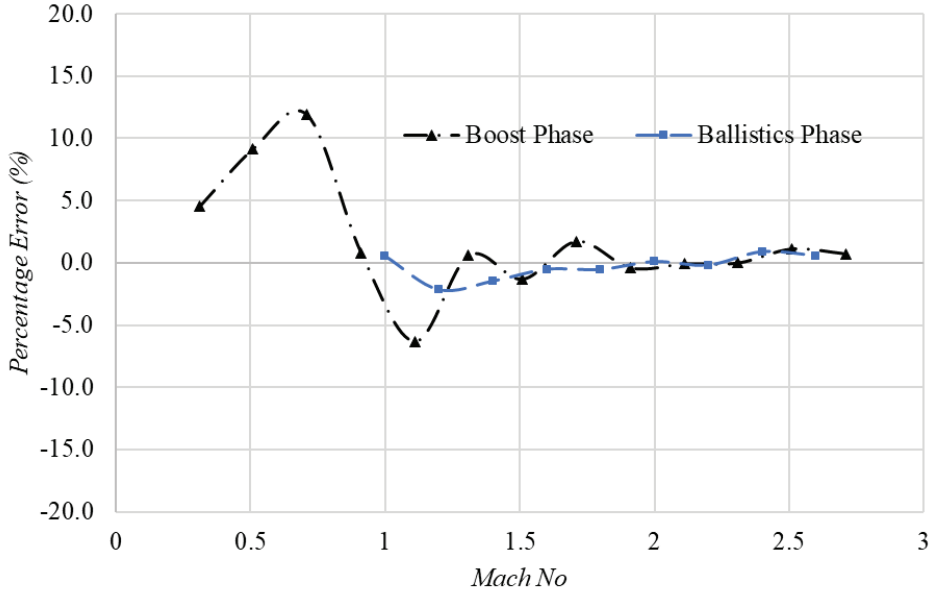

Figure 4. Percentage error drag estimation.

shown in Fig. 4. In the regime of the subsonic boost phase, the error is up to 11% as the filter is not fully converged. Once the filter converges, the error in the boost and ballistics phase is less than 5 %. EKF estimates $C_D = (C_{D_o} - C_{D_{bo}})$ in both the boost and ballistics phases. The boost and ballistics phase drag values are calculated for Mach number for which both the values are estimated and tabulated in Table 2. The average percentage difference is around 29 %. It means that the boost phase drag is 0.71 times the ballistics phase drag.

Table 2. Ballistics and Boost phase difference

Mach No	Ballistics phase drag	Boost phase drag	Percentage difference
1.0	0.577	0.395	31.5
1.2	0.623	0.433	30.5
1.4	0.566	0.410	27.6
1.6	0.509	0.366	28.1
1.8	0.462	0.335	27.5
2.0	0.434	0.313	27.9
2.2	0.422	0.302	28.5
2.4	0.415	0.296	28.7
2.6	0.408	0.293	28.3

3.2 Base Drag of Base Bleed Projectile

As discussed, drag acting during base bleeding is very difficult to obtain as the performance of base bleed depends on ambient atmospheric pressure and spin of projectiles. The burn time also depends on these parameters. In this work, estimation of base bleed drag and burn time is done effectively.

The projectile of 155 mm is considered for simulation. The input and physical properties are listed in Table 1. The trajectory is obtained for muzzle velocity 900 m/s and launch angle 45°. The range of trajectory is 36.2 km, and the attending height is 12.2 km. The time of flight is 102 s. The required trajectory is expressed in terms of a set of measurements. These measurements are passed to the developed EKF model to estimate drag during the base bleed and ballistics phase. We can see that the estimation error is well within theoretical bounds. This indicates that the proposed method is working well. The actual and estimated drag is shown in Fig. 5, and the error in drag coefficients is shown in Fig. 6.

The relation $C_D = (C_{D_o} - f_{d_r} C_{D_{bo}})$ and these computations may provide a correlation of change in the base pressure with mass injection and Mach number by processing multiple trajectories.

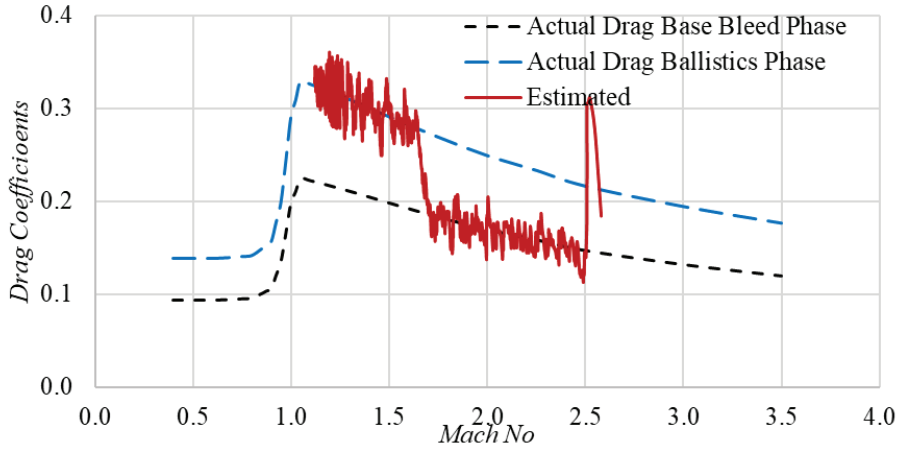

Figure 5. Drag coefficient error w.r.t time.

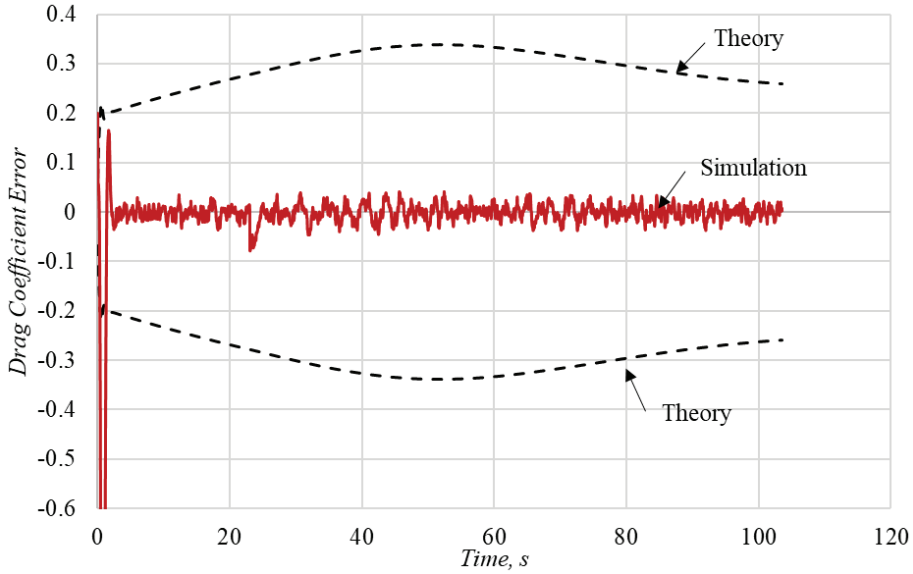

Figure 6. Base bleed and ballistics phase drag estimation.

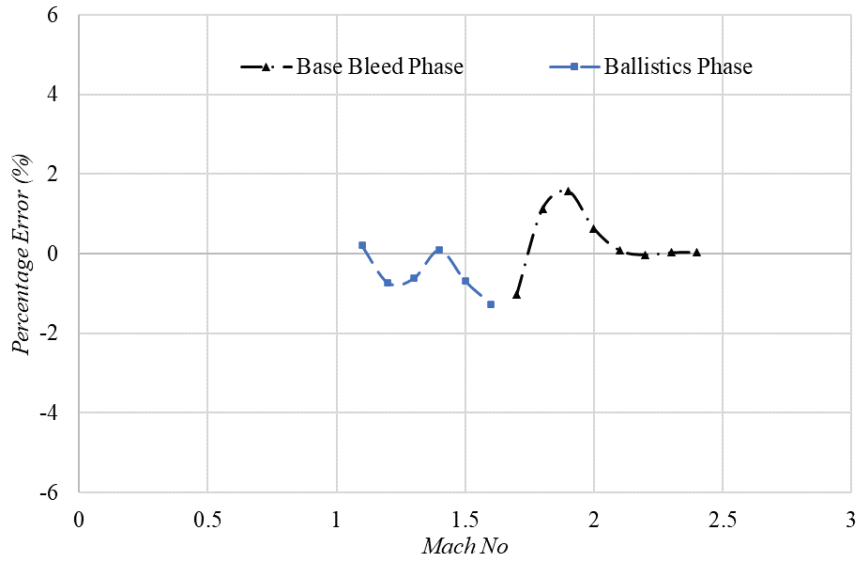

Figure 7. Percentage error drag estimation.

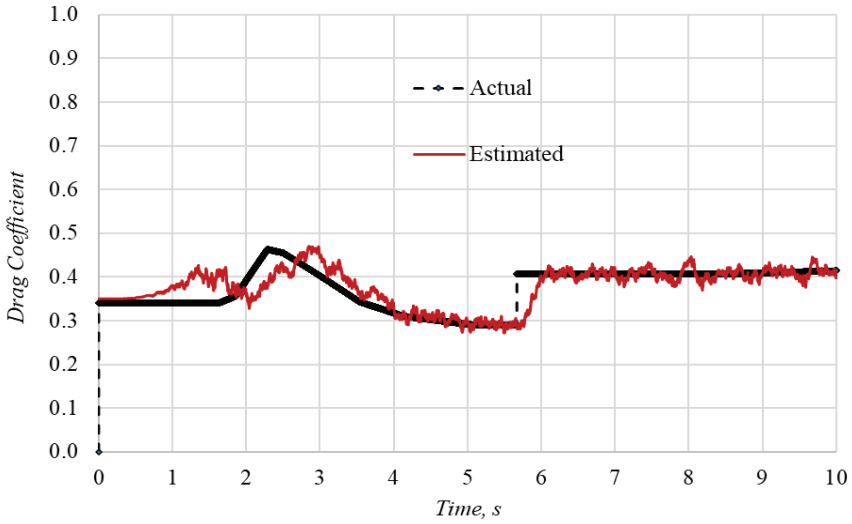

Figure 8. Drag estimation in zoomed view.

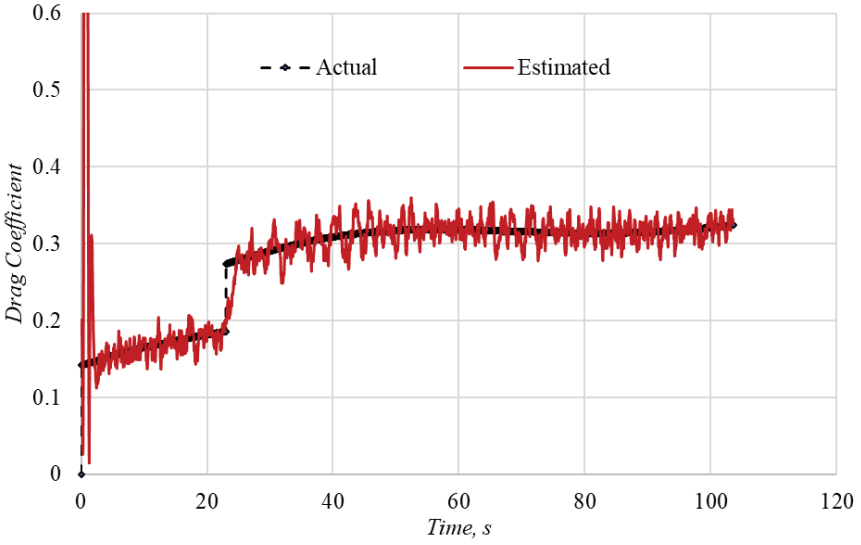

Figure 9. Drag coefficient w.r.t. time.

The percentage error is calculated for the estimated base bleed and ballistics phase drag and is shown in Fig. 7. The error in the base bleed and ballistics phase is less than 5 %.

In the base bleed phase, the Mach number starts at 2.64 and reduces to 1.75 when the base bleed propellent is completely burnt out. After switching to the ballistics phase, it decreases further along with the trajectory. The drag value at the end of the base bleed is 0.184 and just after the base bleed is off is 0.279. It can be inferred that due to base bleed, there is an overall 34 % reduction in drag.

4. BURN TIMEESTIMATION

It is known that during burn of rocket mortar or base bleed the total drag is less than the ballistics phase due to absence or reduction in base drag. It is expected that once burning is over, the total drag will suddenly increase due to the acting of base drag. The sudden change in total drag will be indicated by the gap in the drag profile. It is interesting to note that the filter automatically takes care of both phases. Moreover, if we plot estimated data concerning time then burn time can be estimated by monitoring the sudden change in total drag which is indicated by the gap in the drag profile.

For a 122 mm fin-stabilized rocket the drag coefficient during the boost and ballistics phase is estimated the zoom view is shown in Fig. 8. The EKF switched to the ballistics phase around 5.6. It means that by processing trajectory flight data using EKF, the burn time can be estimated.

For the 155 mm base bleed case, we plotted estimated data concerning time. The sudden change in total drag will be indicated by the gap in the drag profile. In this case, the sudden change occurred at 23 sec. The burn time for the current simulation is 23 sec and it can be inferred from Fig. 9.

The conditions of the firings were controlled by changing elevation and muzzle velocity, weapon altitude, propellant charge, and grain temperature. The separation of these influence parameters is tough. These most influential parameters are highly correlated and cannot be varied independently. For instance, increasing the velocity or the elevation results in a decrease in the mean ambient air pressure on which the base bleed is on.

Spin is the most important parameter affecting the characteristics of burning. Static burning and burning with spin are completely different behaviour. At the moment, there is no complete, satisfactory theory explaining this effect. At high spin rates, due to centrifugal forces, the flames of the reacting gases are closer to the grain surface. It enforces a higher rate of burning[24].

The pressure inside the base bleed unit is related to the outside pressure. Therefore, the burning rate must be a function of the outside air pressure. Measuring burning performance at ambient pressure on the ground is highly tricky and costly.

As discussed previously, measurement of the exact burn time of base bleeding is very difficult since it is depending on the spin rate and ambient atmospheric pressure in which the projectile is flying. To demonstrate the capability of the proposed method to estimate burn time, two cases are simulated. The base bleed conditions are given in Table 3.

Indication of burn time off can be seen in the plot of drag estimation concerning time.

The estimation of the drag coefficient in both cases is within a 95 % confidence level. To find burn time, one needs to observe timing when the filter is switching to ballistics phase drag coefficient. The filter switching timing can be noted when

Table 3. Base bleed conditions

Parameters	Unit	Case I	Case II
Muzzle Velocity	m/s	900	750
Thrust/ Burn Time/	s	23	26
Launch Angle	deg	45	45
Burn end Altitude	m	10000	8000
Pressure at Burn start	hpa	1013.0	1013.0
Pressure at Burn end	hpa	264	356
Spin at the Burn start	rpm	17424	14520
Spin at the Burn end	rpm	15536	13316

Table 4. Estimated burn time and error

Parameters	Unit	Case I	Case II
Actual burn time	s	23.0	26.0
Estimated burn time	s	23.2	26.7
Error	s	0.2	0.7
Percentage error	%	0.9	2.3

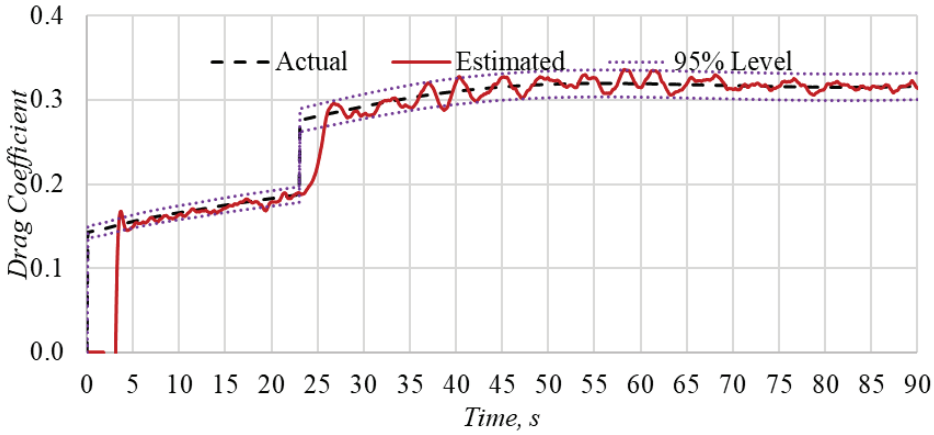

Figure 10. Burn time estimation for higher spin and lower pressure.

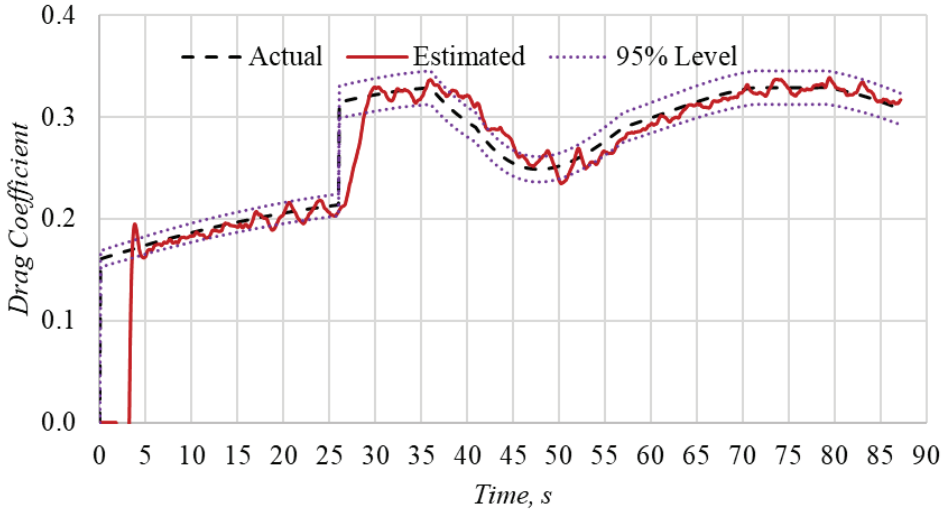

Figure 11. Burn time estimation for lower spin and higher pressure.

there is a sudden increase in drag coefficients as shown in Fig. 10 and Fig. 11 for cases I and II respectively.

We can see in Table 4 that the percentage error in the first case is 0.9 % and in the second case 2.3 %. Burn time estimation is within 5 %.

5. CONCLUSION

Obtaining base drag or base bleed drag or the effect of tracer burning is highly dependent on empirical methods. The mass flow rate is measured at steady conditions, and then it is empirically converted into base drag reduction. In particular, measurement of the burn time of base bleeding is very difficult since it depends on the spin rate and ambient atmospheric pressure in which the projectile is flying. It requires instrumentation and onboard sensor, ground telemetry to measure these parameters. Due to space constraints and high g launching accelerations, survival of the on-board sensor itself is a challenging task. In this paper, trajectory flight data is used to estimate base drag and indirect measurement of burn time. An estimation of both base drag and burn time is within 5 % accuracy. The simulation is carried out for two configurations, artillery shell and rocket. The proposed method works well for both conditions. Exhaustive simulation results indicate that the method can be used for any configuration.

No special measurements are needed other than trajectory data for this estimation. The proposed methods are simple, useful, and cost-effective. Estimation by other methods requires explicit trials, large infrastructure, and higher costs. The proposed methods can be used as effective tools for post-trial analysis too. An estimation by these methods can be used to compare estimations by other methods or direct measurement or experimental results. The proposed method can be enhanced if all the other aerodynamic coefficients are known. In this case, the highly nonlinear and coupled trajectory model, i.e., six-degree freedom, can be used as a system dynamics filter. EKF can be replaced with an Unscented Kalman Filter or Particle filter to remove first-order linearization of the nonlinear system dynamics and to cater for non-Gaussian noise.

REFERENCES

1. Reddy, D. Siva Kishna; Sah, P.K. & Sharma, Ashish. Prediction of drag coefficients of a base bleed artillery projectile at supersonic Mach number. *J. Physics: Conference Series*, 2021, **2054**. doi:10.1088/1742-6596/2054/1/012013
2. Regodic, D.; Jevremovic, A. & Jerkovic, D.D. The prediction of axial aerodynamic coefficient reduction using base bleed. *Aerospace Sci. Technol.*, 2013, 24-29. doi:10.1016/j.ast.2013.09.001
3. Moss, G.M.; Leeming, D.W. & Farrar, C.L. Military ballistics. *Oxford: Brassey's (UK) Ltd*, 1995. pp. 84-85
4. Zaki, A.; Abdel-Kader, M. & Yakout, H. Performance of artillery projectiles with base bleed unit. *In* 8th International Conference on Aerospace Sciences & Aviation Technology, Cairo, 1999, 1-14. doi:10.21608/ASAT.1999.24873
5. Crewther, I. A complete semi-empirical base bleed model. *In* 18th International Symposium on Ballistics, San Antonio, 1999.
6. Kubberud, N. & Oye, I.J. Extended range of 155 mm projectile using an improvised base bleed unit: simulations and evaluation. *In* 26th International Symposium on Ballistics, Miami, 2011. http://proceedings.ndia.org/1210/12015.pdf (Accessed on 12 December 2020).
7. ESDU 00017. Supersonic base and boat-tail pressure drag of cylindrical bodies with a conical boat-tail and a central propulsive jet. *ESDU*, 2000.
8. Hymer, Moore F.G. & Thomas, C. Improved power-on base drag methodology for the aero prediction code. *Naval Surface Warfare Center*, Dahlgren, 2001. https://apps.dtic.mil/sti/pdfs/ADA390967.pdf (Accessed on 18 October 2019).
9. Aziz, M.M.; Ibrahim, A.Z.; Ahmed, M.Y.M and Riad, A.M. Multi-fidelity drag prediction for base bleed projectile. *In* IOP Conference Series: Material Science and Engineering, 2020. doi:10.1088/1757-899X/973/1/012033

10. Singh, S. & Ghosh, A.K. Parameter estimation from flight data of a missile using maximum likelihood and neural network method. *In* AIAA Atmospheric Flight Mechanics Conference and Exhibit, Keystone, Colorado, 2006. doi:10.2514/6.2006-6284.
11. Zhang, J.; X. Wang, & Yao, J. Coefficient identification of trajectory correction fuze based on sensitivity function. *In* 5th IEEE Conference on Industrial Electronics and Applications, 2010, 789-792, doi: 10.1109/ICIEA.2010.5515069
12. Chen, Y.; Wen, C.; Gong, Z. & Sun, M. Drag coefficient curve identification of projectiles from flight tests via optimal dynamic fitting. *Control Engineering Practice*, 1997, **5**(5), 627-636, doi:10.1016/S0967-0661(97)00044-0
13. Chen, Y.; Wen, C.; Dou, H. & Sun, M. Iterative learning identification of aerodynamic drag curve from tracking radar measurements. *Control Eng. Pract.*, 1997, **5**(11), 1543-1553. doi: 10.1016/S0967-0661(97)10008-9
14. Chen, Y.; Wen, C.; Xu, J.X. & Sun, M. High-order iterative learning identification of projectile's aerodynamic drag coefficient curve from radar measured velocity data. *IEEE Transact. Control Syst. Technol.*, 1998, **6**(4), 563-570, doi: 10.1109/87.701354
15. Chun,WeiHuang; Chun, Liang Lin & Yu, Ping Lin. Estimator design for re-entry targets. *ISA Transactions*, 2014, **53**, 658–670, doi:10.1016/j.isatra.2013.11.010
16. Zhou, P.; Shen, Q.; Li, D.G. & Yang, D.H. A method of trajectory estimation and prediction using extended Kalman filter based on GPS data. *In* 27th International Symposium on Ballistics, Freiburg, Germany, 2013.
17. Lin, Y.P.; Lin, C.L.; Huang, C.W. & Chen, Y.Y. Trajectory estimation of higher-tier ballistic targets. *In* 8th Asian Control Conference (ASCC), Kaohsiung, Taiwan, 2011, 476-481. INSPEC Accession Number: 12072562
18. Zhou, W. An improved hybrid extended Kalman filter based drag coefficient estimation for projectiles. *In* 30th International Symposium on Ballistics, Long Beach, CA, 2017. doi: 10.12783/ballistics2017/16782
19. Coleman, N.; Yip, P. & May, R. Wind profile extraction and impact point prediction from projectile trajectory measurements. Proceedings of the American Control Conference, San Diego, California, 1999, **3**, 1915-1919. doi: 10.1109/ACC.1999.786186
20. Gite, L.K. & Deodhar, R.S. Estimation of yaw angle from flight data using extended Kalman filter. *Aerospace System*, 2022, 393-402. doi:10.1007/s42401-022-00131-3
21. Gite, L.K.; Anandaraj, A.; Padmanabhan, M. & Rajan, K.M. Adaption of modified point mass model for efficient trajectory parameters computation of artillery rockets. *In* 31st International Symposium on Ballistics, Hyderbad, 2019. doi: 10.12783/ballistics2019/33110
22. Shyam, Mohan M.; Naren, Naik; Gemson, R.M.O. & Ananthasayanam, M.R. Introduction to the Kalman filter and tuning its statistics for near optimal estimates and Cramer Rao bound. IIT, Kanpur, 2015. http://home.iitk.ac.in/~nnaik/pdf/shyammohantr.pdf (Accessed on 10 January 2020).
23. Chhabra, A.; Venepally, J.R & Kim, D. Measurement noise covariance adapting Kalman filters for varying sensor noise situations. *Sensors*. 2021, **21**(24):8304 doi: 10.3390/s21248304
24. Gliga, L.I.; Chafouuk, H; Popescu, D. & Lupu, P. A method to estimate process noise covariance for a certain class of nonlinear systems. *Mech. Syst. Signal Process.* 2019, **131**, 381-393. doi: 10.1016/j.ymssp.2019.05.054
25. Balon, R. & Komenda, J. Analysis of the 155 mm ERFB/BB projectile trajectory. *Advances in MT*, 2006, **1**(1), 91-114. https://www.aimt.cz/index.php/aimt/article/view/1718 (Accessed on 10 January 2020).

CONTRIBUTORS

Dr L.K. Gite obtained his PhD in parameter estimation and working as a Scientist at DRDO-ARDE, India. His research interests include: External ballistics, aerodynamics, and parameter estimation.
In the current study, he proposed the methodology and simulate edit to estimate the base drag coefficients. The data analysis and manuscript writing were carried out by him.

Dr R.S. Deodhar obtained PhD from IIT, Mumbai and is working as a Scientist at DRDO-ARDE, Pune. His research interests include: Statistical analysis, external ballistics parameter estimation, and quality and reliability.
In the current study, he contributed to simulating different configurations so that the proposed methodology becomes robust. He also supervised the complete work, framing it into a research article, and carried out manuscript editing.